**Key Points:**
- Overland-flow connectivity occurs along an ephemeral drainage network
- Connectivity is nonlinearly related to catchment response
- The connectivity concept could be used for catchment classification

**Supporting Information:**
- Description of supplementary material
- Evidence for the occurrence of overland flow
- Figures S1, S2, S3, S4, S5

**Correspondence to:**
B. Zimmermann,
b.zimmermann@fib-ev.de

# Connectivity of overland flow by drainage network expansion in a rain forest catchment

**Beate Zimmermann[1,2], Alexander Zimmermann[1], Benjamin L. Turner[3], Till Francke[1], and Helmut Elsenbeer[1,3]**

[1]Institute of Earth and Environmental Sciences, University of Potsdam, Potsdam, Germany, [2]Now at Research Institute for Post-Mining Landscapes, Finsterwalde, Germany, [3]Smithsonian Tropical Research Institute, Panama City, Panama

**Abstract** Soils in various places of the Panama Canal Watershed feature a low saturated hydraulic conductivity ($K_s$) at shallow depth, which promotes overland-flow generation and associated flashy catchment responses. In undisturbed forests of these areas, overland flow is concentrated in flow lines that extend the channel network and provide hydrological connectivity between hillslopes and streams. To understand the dynamics of overland-flow connectivity, as well as the impact of connectivity on catchment response, we studied an undisturbed headwater catchment by monitoring overland-flow occurrence in all flow lines and discharge, suspended sediment, and total phosphorus at the catchment outlet. We find that connectivity is strongly influenced by seasonal variation in antecedent wetness and can develop even under light rainfall conditions. Connectivity increased rapidly as rainfall frequency increased, eventually leading to full connectivity and surficial drainage of entire hillslopes. Connectivity was nonlinearly related to catchment response. However, additional information on factors such as overland-flow volume would be required to constrain relationships between connectivity, stormflow, and the export of suspended sediment and phosphorus. The effort to monitor those factors would be substantial, so we advocate applying the established links between rain event characteristics, drainage network expansion by flow lines, and catchment response for predictive modeling and catchment classification in forests of the Panama Canal Watershed and in similar regions elsewhere.

## 1. Introduction

Overland flow (surface runoff) occurs when intense rain falls onto a soil of low infiltrability, or where ground or soil water intersects the soil surface. The first situation gives rise to infiltration-excess or Horton overland flow (HOF), while extremely wet conditions may result in saturation-excess overland flow (SOF) or return flow (RF). These mechanisms of overland-flow generation can be tightly linked: SOF and RF, for instance, were reported to coexist in some catchments [*Elsenbeer and Vertessy*, 2000; *Sayer et al.*, 2006].

Regardless of the type of overland flow, it is increasingly recognized that its mere documentation cannot explain whole watershed behavior, because surface runoff may or may not be captured by the channel system; reinfiltration reduces the significance of overland flow for water and solute fluxes. This awareness raised the desire to track the fate of a flow path and added to the popularity of the concept of connectivity [*Bracken and Croke*, 2007; *Lane et al.*, 2009; *Michaelides and Chappell*, 2009; *Ali and Roy*, 2010; *Wainwright et al.*, 2011]. In search of explanations for watershed functioning, the connectivity between runoff generated on hillslopes and channel flow is of paramount importance and is likewise captured by the term hillslope-channel coupling [*Brunsden and Thornes*, 1979; *Michaelides and Wainwright*, 2002]. Connectivity of overland flow—as opposed to connectivity of subsurface flow—can be assessed relatively easily, because the vectors of flow concentration for surface runoff are often known. In a semiarid area prone to HOF, for instance, connectivity develops in nonvegetated patches that serve as connectivity bands [*Mueller et al.*, 2007]. In other areas, roads and footpaths create hydrologic connectivity [e.g., *Ziegler et al.*, 2001; *Hölzel and Diekkrüger*, 2012]. In contrast, flow paths are less obvious in catchments where subsurface flow dominates and the monitoring of connectivity either involves substantial hydrometric instrumentation (e.g., 135 crest stage gauges and 29 recording wells in *Tromp-van Meerveld and McDonnell* [2006b] or 84 wells in *Jensco et al.* [2009]), or many multiple-depth soil moisture measurements [*Ali and Roy*, 2010].

For both surface and subsurface flow, an investigation of flow path connectivity across entire hillslopes or catchments often aims to understand nonlinear rainfall-runoff relationships. Here, the concept of

connectivity promises to merge different flow processes into an index that explains where and when flow is connected [*Jensco et al.*, 2009]; as stated above, any flow path becomes irrelevant if it lacks connectivity. In Japanese forest plantations, for instance, no significant correlation was found between the amount of overland flow and direct runoff from catchments [*Gomi et al.*, 2010], which indicates little coupling between overland flow generated on hillslopes and the channel system. Connected flow, in contrast, influences hillslope and catchment runoff as well as sediment and solute export, as was shown for stormflow at the hillslope [*Tromp-van Meerveld and McDonnell*, 2006a, 2006b] and catchment [*Jensco et al.*, 2009] scales, and for solute transport [*Ocampo et al.*, 2006; *Frey et al.*, 2009]. This link between connectivity and hillslope or catchment response is not universal, however, since connectivity is system-specific and time-variant depending on factors such as antecedent wetness conditions and rain event characteristics [*Bracken and Croke*, 2007; *Jensco et al.*, 2009]. For instance, subsurface flow systems often require rainfall or storage thresholds to be exceeded before flow connection occurs [*Ocampo et al.*, 2006; *Tromp-van Meerveld and McDonnell*, 2006a; *McGuire and McDonnell*, 2010]. Likewise, antecedent conditions can have a large impact on spatial patterns of infiltration and runoff production and, hence, connectivity [*Bracken and Croke*, 2007]. While overland flow on a hydrophobic soil occurred preferentially during drought conditions [*Buttle and Turcotte*, 1999], large antecedent wetness gave rise to SOF even for small rainfall rates in a rain forest catchment featuring a low permeability at shallow depth [*Bonell et al.*, 1979]. These examples suggest that the dynamic component of connectivity is of limited transferability, as it depends on a catchment's runoff regime.

Despite the great attention given to the various facets of hydrological connectivity, only a few studies have thoroughly investigated its nature, drivers, and consequences. In other words, there is a mismatch between conceptual progress and field evidence. In addition, the available case studies have focused on subsurface stormflow and groundwater flow in humid regions [*Ocampo et al.*, 2006; *Jensco et al.*, 2009; *Tromp-van Meerveld and McDonnell*, 2006b; *McGuire and McDonnell*, 2010], or on infiltration-excess overland flow [*Gomi et al.*, 2010; *Sen et al.*, 2010]. Few studies have focused on hillslope-channel coupling in catchments featuring SOF, RF, or both, which is unfortunate given the hypothesized tight coupling of hillslope and channel processes in these environments [*Elsenbeer and Vertessy*, 2000; *Sayer et al.*, 2006]. For instance, *Zimmermann et al.* [2012] reported high rates of suspended sediment leaving a forested catchment subject to frequent overland flow, which they partly attributed to an effective connection between hillslopes and streams. Their suspicion is further supported by the preferred occurrence of overland flow at certain microtopographical positions, most notably concentrated flow lines [*Loos and Elsenbeer*, 2011] that all drain into the channel network of the catchment.

To provide evidence for the hypothesized hillslope-channel coupling by flow lines, we designed a monitoring study to answer the following questions: (1) How does connectivity in flow lines develop?, (2) What are the meteorological conditions?, (3) How does connectivity influence storm runoff, suspended sediment, and total phosphorus export?. These questions are of interest to a range of scientific disciplines and have important implications for water quality [*Brauman et al.*, 2007]. Given this socio-economic relevance, we use the findings of our field experiment to conceive of potential applications of the connectivity concept for catchment classification and management.

## 2. Methods

### 2.1. Study Site

The 3.3 ha Lutzito catchment is located on Barro Colorado Island, Panama (9° 9′ 32″ N, 79° 50′ 17″ W; Figures 1a–1c). The island was isolated from the mainland in 1914 after the Chagres River was dammed to form Lake Gatun, which is part of the Panama Canal. The topography of Lutzito catchment is heterogeneous: many small channels and rills dissect slopes that reach 35° in places.

Barro Colorado supports tropical semideciduous lowland forest [*Foster and Brokaw*, 1982]. The forest in Lutzito catchment (Figure 1c) is secondary growth >130 years old [*Kenoyer*, 1929]. Stand height is 25–35 m with a few emergent trees approaching 45 m. A vegetation survey in Lutzito catchment, considering stems >5 cm diameter at breast height, revealed that a single hectare contains approximately 98 tree species and 1140 stems, with a total basal area of 35 $m^2$ $ha^{-1}$ [*Zimmermann et al.*, 2009].

The climate is strongly seasonal, with a wet season that usually lasts from May to mid-December. Annual rainfall averages 2641 ± 485 mm (mean ± 1 sd, $n = 82$, data from 1929 to 2010; data from the
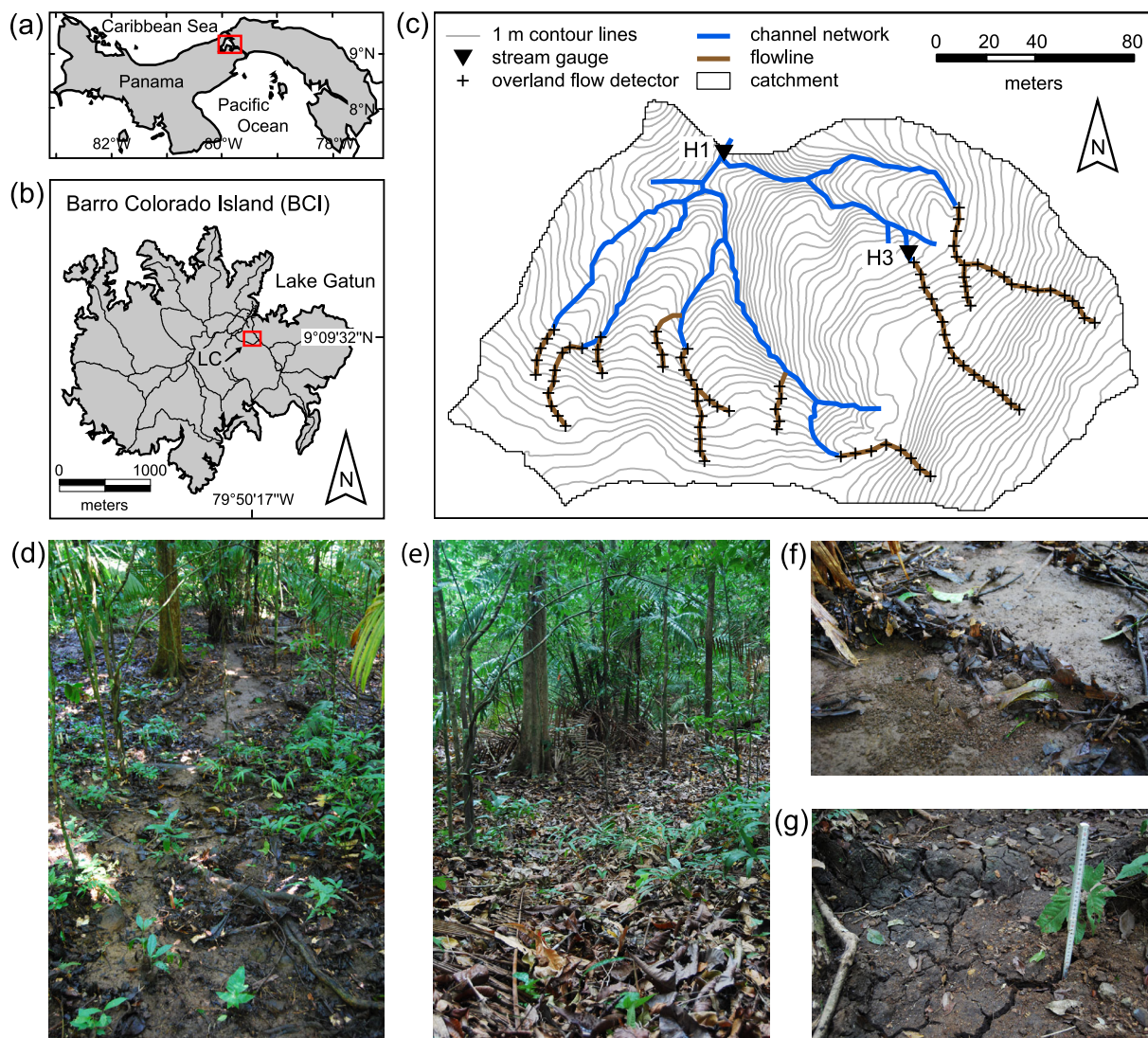
**Figure 1.** Location of the research area in (a) Panama and (b) on Barro Colorado Island. (c) Map of the Lutzito catchment (LC) that shows the channel system, position of flow lines, and locations of overland-flow detectors and discharge monitoring sites. Note that back-up OFDs are not displayed. (d) A view of flow line #2 near the gauging site during the late rainy season. (e) Photograph of the same flow line at the end of the dry season. (f) Close-up of the soil surface in a flow line; dams of sediment and leaf litter indicate active surficial processes. (g) Soil cracks in a flow line at the end of the dry season; the photograph was taken after the removal of a thick layer of leaf litter.

Environmental Sciences Program, Smithsonian Tropical Research Institute, Republic of Panama). Long-term averages of monthly rainfall indicate a fairly uniform rainfall distribution during the wet season, with a maximum of 400 mm in November. However, interannual variation of monthly rainfall is substantial, with common pronounced dry spells during the wet season.

The Lutzito catchment is underlain by tuffaceous siltstone of the Caimito Marine Facies [*Woodring*, 1958]. Soils are classified as Eutric Cambisols [*FAO*, 1998] or, following USDA criteria [*Soil Survey Staff*, 2006], as Typic Eutrudepts [*Baillie et al.*, 2007]. Soil depth varies between 0.3 m on some ridges and steep slopes and ~1 m elsewhere. At the end of the dry season (May), and to a lesser extent during prolonged dry periods (June–July), soils in the Lutzito catchment develop cracks up to 2 cm wide and 10 cm deep (Figure 1g) due to a substantial admixture of smectite in the clay fraction [*Grimm et al.*, 2008]. During the progressing wet season, cracks close and relative water saturation in the upper soils increases to >60% [*Zimmermann et al.*, 2012]. The infiltrability far exceeds rainfall intensities (Table 1), but there is evidence for a strong decrease of the saturated hydraulic conductivity ($K_s$) at a shallow depth (Table 1), which suggests the occurrence of saturation-excess overland flow (SOF).

**Table 1.** Summary of Infiltrability and Saturated Hydraulic Conductivity ($K_s$) Data From the Lutzito Catchment

| Depth (cm) | Infiltrability/$K_s$ (mm h$^{-1}$) | | | Sample Size | Reference |
| --- | --- | --- | --- | --- | --- |
| | LQ[a] | Median | UQ[b] | | |
| 0 | 208.4[c] | 406.9[c] | 525.0[c] | 18 | Zimmermann et al. [2012] |
| 0–6 | 5.5[d] | 71.6[d] | 312.8[d] | 118 | Zimmermann et al. [2013] |
| 6–12 | 0.8[d] | 7.3[d] | 44.2[d] | 111 | Zimmermann et al. [2013] |
| 12.5 | – | 29.7[e] | – | 74 | Godsey et al. [2004] |
| 30 | – | 1.4[e] | – | 40 | Godsey et al. [2004] |

[a]Lower quartile.
[b]Upper quartile.
[c]Infiltrability measured with a hood infiltrometer (UGT, Müncheberg, Germany).
[d]$K_s$ measured with cores of 7.3 cm diameter.
[e]$K_s$ measured with a constant head permeameter; measurements were conducted during the dry season, which partly explains the somewhat larger values compared to the data from Zimmermann et al. [2013].

Several studies reported the frequent occurrence of overland flow in the Lutzito catchment [*Godsey et al.*, 2004; *Zimmermann et al.*, 2012], which dominates the runoff response. Return flow (e.g., from soil pipes) also constitutes a source of overland flow in the Lutzito catchment (A. Zimmermann, unpublished data), though its contribution to runoff remains unknown [*Kinner and Stallard*, 2004].

As mentioned earlier, overland flow in our research catchment tends to concentrate in flow lines [*Loos and Elsenbeer*, 2011]. Flow lines are microtopographic elements on hillslopes which feature particularly low $K_s$ [*Zimmermann et al.*, 2013] and extend the channel network (Figures 1c–1d). Though overland flow occurs most frequently in flow lines, surface runoff is not restricted to them [cf. *Loos and Elsenbeer*, 2011, Figure 3]. Particularly during large rain events, the vicinity of flow lines and other microtopographic positions such as swales also contribute to surface runoff [see *Zimmermann et al.*, 2012, 2013, supporting information and video material].

None of the Lutzito catchment's channels has perennial flow: base flow in the main channel ceases during the dry season, and flow in most tributary channels is either seasonal or ephemeral. In addition, riparian zones do not exist, an advantageous condition for studying hillslope-channel connectivity [*McGuire and McDonnell*, 2010].

The occurrence of low $K_s$ values at a shallow depth and the occurrence of overland flow in undisturbed forest of the Panama Canal Watershed are not restricted to the geological formation of our study site. In fact, several studies in parts of the Panama Canal Watershed underlain by igneous bedrock (e.g., andesite and basalt) have reported a pronounced decline in soil permeability with depth [*Godsey et al.*, 2004; *Hendrickx et al.*, 2005; *Hassler et al.*, 2011]. Two of the latter studies also mention observations of overland flow [*Godsey et al.*, 2004; *Hassler et al.*, 2011] (see also supporting information).

### 2.2. Field Data
### 2.2.1. Rainfall Data
Rainfall was recorded with a tipping bucket in 5 min resolution in a clearing 250 m away from our study site (data by courtesy of the Environmental Sciences Program, Smithsonian Tropical Research Institute, Republic of Panama). Because tipping bucket measurements ($N_{bucket}$) usually underestimate high-intensity rainfall, we used complementary bulk rainfall data of daily resolution ($N_{total}$, $n = 2825$ days) for the correction of the tipping bucket record ($N_{corrected}$). Assuming that underestimation starts at a threshold amount per time step ($N_{thresh}$), above which the measurement error increases linearly with $c$, we optimized equation (2) for $N_{thresh}$ and $c$ to match the daily rainfall record:

$$\sum_{i=1}^{t_{step}} N_{corrected}\,(\text{day}\,,i) \overset{!}{=} N_{total}\,(\text{day}\,) \tag{1}$$

$$N_{corrected}\,(\text{day}\,,i) = N_{bucket}\,(\text{day}\,,i) + \max\,(0, N_{bucket}\,(\text{day}\,,i) - N_{thresh}\,) \cdot c \tag{2}$$

where $t_{step}$ refers to the number of time steps per day.
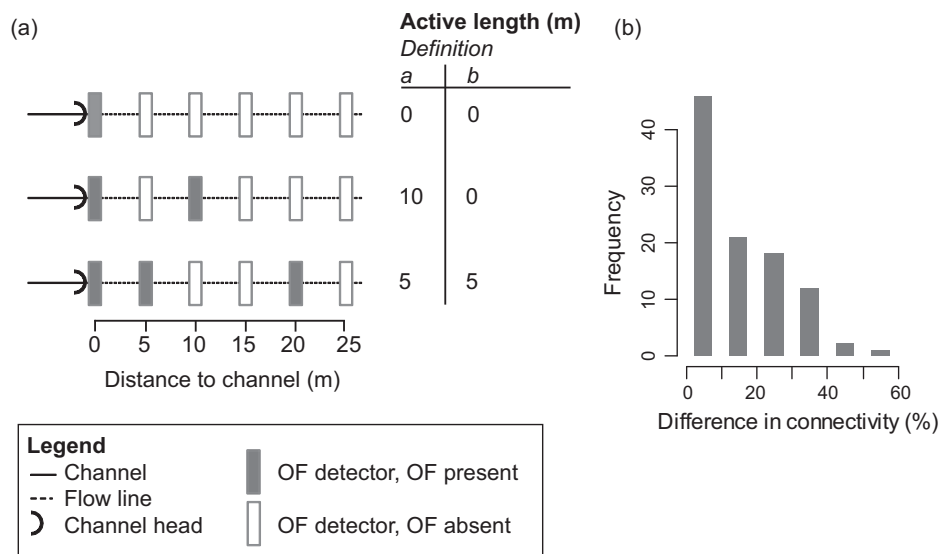
**Figure 2.** Source and consequences of uncertainty in the determination of the active length of a flow line from overland-flow recordings: (a) the two possibilities for handling of the full-empty-full situation when determining the active length and (b) resulting differences between the two possible results for our event-based connectivity index. Note that flow lines flow into channels at many possible locations, one of which is the channel head.

Based on the corrected tipping bucket data we selected rain events, which are defined as rainfall periods separated by at least 2 h without rainfall. This rain-event data set provided the basis to identify the most important rainfall parameters and antecedent wetness indices for the development of connectivity in the Lutzito catchment (section 2.3.2).

### 2.2.2. Monitoring of Overland-Flow Occurrence

During three consecutive rainy seasons (2007–2009), we monitored the occurrence of overland flow during rainfall events exclusively in flow lines (Figure 1c). We restricted the monitoring to flow lines because in our research area flow lines represent the dynamic component of the drainage network, whereas the channel network responds to all but the smallest rain events (A. Zimmermann, unpublished data). To monitor overland flow, we installed overland-flow detectors (hereafter OFDs), modified after *Kirkby et al.* [1976]. The monitoring started in flow lines that we had identified in the field during rain events; over the years, ever increasing field knowledge enabled us to identify and instrument all major flow lines. The OFDs were installed within each flow line at regular distances of 5 m (Figure 2a). Depending on the location of a particular flow line's outlet, we placed the first detector either just above the channel head or directly adjacent to the channel or the main flow line (Figure 1c). A flow line's upslope origin marked the position for a flow line's last OFD, which was near the catchment divide in some cases (Figure 1c). The total number of OFDs per flow line varied as a function of flow line length (Figure 1c). We checked OFD responses no earlier than 2 h after the end of a rainfall event; in doing so, we assumed that overland flow had occurred only if the collecting container was entirely filled with water,
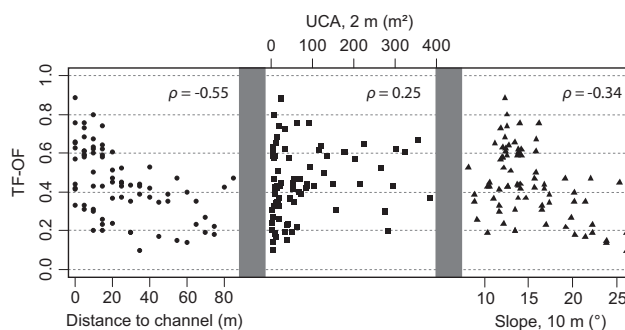


**Figure 3.** The dependence of the temporal frequency of overland-flow occurrence (left) on the distance-to-channel as measured in the field, (middle) on the upslope contributing area calculated with the single flow path algorithm from a DEM of 2 m resolution, and (right) on the slope derived from a DEM of 10 m resolution; $\rho$ is Spearman's rank correlation coefficient. The attribute flow path length as derived from the 5 m resolution DEM and the distance-to-channel measure gave a very similar value of $\rho$. Correlations between TF-OF and all other combinations of terrain attributes, DEM resolutions, and algorithms were weaker than those referred to above.

**Table 2.** Summary Statistics of Rainfall Parameters of the Monitored Events[a]

| Quartile | Total Rainfall (mm) | Max$_{I5}$[b] (mm/h) | Max$_{I30}$[c] (mm/h) | Max$_{I60}$[d] (mm/h) | Duration[e] (min) | API$_1$[f] (mm) | API$_{16}$[g] (mm) | API$_{128}$[h] (mm) |
|---|---|---|---|---|---|---|---|---|
| Minimum | 0.6 (0.3) | 3.5 (3.5) | 0.6 (0.6) | 0.3 (0.3) | 15 (5) | 0.0 (0.0) | 20.2 (9.0) | 366.4 (252.6) |
| Median | 12.4 (4.3) | 38.1 (17.3) | 17.9 (6.4) | 10.3 (3.5) | 140 (85) | 1.3 (2.3) | 117.2 (144.7) | 886.0 (1152.4) |
| Maximum | 100.2 (110.0) | 204.4 (204.4) | 136.9 (136.9) | 84.6 (84.6) | 740 (830) | 49.4 (100.5) | 345.0 (416.6) | 1424.7 (1582.9) |

[a]Values in parentheses refer to all events in the three monitored rainy seasons (June–December 2007, 2008, 2009), one-tip "events" are excluded.
[b]Maximum 5 min rainfall intensity.
[c]Maximum 30 min rainfall intensity.
[d]Maximum 60 min rainfall intensity.
[e]Event duration.
[f]24 h antecedent precipitation index.
[g]16 days antecedent precipitation index.
[h]4 months antecedent precipitation index.

which yields a conservative estimate of overland-flow frequency. If the subsequent event started during sampling, we excluded the actual event from the analysis. In total, we successfully sampled 98 rainfall events whose magnitude varied between less than 1 and 100 mm (Table 2). By sampling as many events as possible, we were able to exhaustively sample the local rainfall distribution in the monitoring period (Table 2).

### 2.2.3. Discharge Measurements, Suspended Sediment Sampling, and Total Phosphorus Determination

We monitored discharge and collected water samples at five sites in the Lutzito catchment [*Zimmermann et al.*, 2012]. Here, we focus on two data-rich sites (Figure 1c): the catchment outlet (H1, 3.3 ha) and a site which solely received overland flow (H3, 0.08 ha). We equipped the sites H1 and H3 with a 2 ft and a 1 ft H-flume, respectively. At each site, we recorded the water level at 5 min intervals with a bubbler flow module (ISCO 730) and a capacitive water stage sensor (Trutrack WT-HR). To ensure constant quality of the discharge record, all instruments were calibrated weekly. Discharge monitoring at H1 started in October 2007, at H3 we began the monitoring in early 2008.

For within-event streamflow sampling, we employed automatic water samplers (ISCO 6712). Occasionally, however, we also took grab samples to cover base flow, to improve coverage early on the rising limb, and to ensure sampling of multiple storms. To adequately sample the flashy streamflow response, we set the trigger for automatic sampling at relatively low discharges and sampled every 5 min for the first hour of an event, then 10 times in 10 min intervals, and finally ended sampling with a 60 min interval. All sediment samples were filtered through preweighed glass fiber filters with a nominal pore size of 1.6 $\mu$m (Whatman, GF/A). Immediately after sampling, we cooled an aliquot to 4°C. Total phosphorus concentration (TP) was determined on unfiltered samples by a persulfate oxidation procedure [*Rowland and Haygarth*, 1997], with phosphate detection by automated molybdate colorimetry on a Lachat Quikchem 8500 (Hach Ltd., Loveland, CO). The detection limit was approximately 0.005 mg P L$^{-1}$. More details on suspended sediment and TP data can be found in Table 3.

### 2.3. Data Analysis
### 2.3.1. Identification of the Mechanism of Connectivity Development

Besides microtopography, terrain attributes such as slope and distance-to-channel measures also exert some control on the temporal frequency of overland-flow occurrence in the Lutzito catchment [*Loos and*

**Table 3.** Characteristics of Suspended-Sediment Concentration (SSC) and Total Phosphorus Concentration (TP) Data

| | SSC | TP |
|---|---|---|
| Sample size | 1675 | 243 |
| Number of events | 71 | 11 |
| Unit | g L$^{-1}$ | mg L$^{-1}$ |
| Minimum | 0.00 | 0.017 |
| Mean | 0.34 | 0.233 |
| Maximum | 2.99 | 1.040 |

*Elsenbeer*, 2011]. This suggests, in line with our field observations, that flow lines connect in a nonrandom fashion, i.e., flow line segments close to the channel network ought to be active earlier than those further away. To test this assumption, we first calculated the temporal frequency of OF occurrence (TF-OF) in flow lines separately for each monitoring location by counting the number of times each overland-flow detector recorded overland flow and then dividing by the total number of monitored events. Next, we calculated Spearman's rank correlation coefficients to evaluate the link between TF-OF and several terrain attributes. One such attribute was the distance-to-channel measure, which we obtained at each OFD location in the field. In addition, we considered several DEM-derived attributes, namely slope, flow path length, upslope contributing area, and the topographic wetness index. For this purpose, we tested DEM resolutions of 1, 2, . . .,10 m; the attributes upslope contributing area and topographic wetness index were further calculated both with a single and a multiple flow path algorithm.

### 2.3.2. Derivation of a Connectivity Index
Our monitoring of overland-flow occurrence generated a nominal variable, i.e., the presence or absence of overland flow at each monitored flow line location. Our aim was then to collapse this information into an index that characterizes the connectivity state of the entire catchment for a given rainfall event. We call this index the "overall event-based connectivity" (hereafter abbreviated with "connectivity"), $C$, which is calculated as follows:

$$C = \frac{\sum_{i=1}^{n} AL_i}{TFL} \tag{3}$$

with $AL_i$ being the active length of flow line $i$, i.e., the part of the flow lines that delivers overland flow to the channel network (Figure 2a), and TFL being the total length of all monitored flow lines. This approach strongly resembles the calculation of drainage density, with the only difference that connectivity is scaled to the length of the flow line system instead of catchment area (the latter would have been possible only if we had measured channel connectivity too); hence, both measures scale linearly. In the Lutzito catchment, the drainage density provided by the channels is 0.019 m/m$^2$ and increases to 0.031 m/m$^2$ if all flow lines contribute to runoff across their entire lengths. In other words, in these full-connectivity situations drainage density rises by 63%.

The determination of the active length of a flow line involves two sources of uncertainty: first, we had to decide on the handling of one empty OFD between two full OFDs, which we call the "full-empty-full" situation. At first sight, it may seem acceptable to stop summing up for active length as soon as there is one empty collector. In practice, however, "false-empty" situations occur due to slight shifts of flow line position [*Zimmermann et al*., 2013] as evidenced by overland flow bypassing an OFD but not its backup; in fact, full-empty-full situations could be attributed to flow line shifting in the majority of cases. We, therefore, preferred an active-length definition that allows for one empty collector between two full ones (Figure 2a, definition *a*). Even so we cannot rule out actual overland-flow discontinuity; thus, the absolute error in the inferred active length per flow line can be as large as 10 m (Figure 2a). If the full-empty-full situation occurs for various flow lines within a given rainfall event, this uncertainty in active-length determination propagates into uncertainty in the calculated overall connectivity. In the majority of cases, the difference in overall connectivity between the two possible definitions remains below 10% (Figure 2b), particularly for low-connectivity events. However, larger differences may occur (Figure 2b). An increasing number of backup OFDs in the course of monitoring helped to reduce this type of uncertainty. Moreover, we explicitly accounted for it in figures that display the original data. During modeling, however, we solely worked with connectivity definition *a* and only implicitly accounted for input data uncertainty (cf. section 2.5.2).

The second source of uncertainty in active length calculation is due to the 5 m distance between adjacent collectors, i.e., we do not know if overland flow stopped 0.1 or 4.9 m after the last full collector. When it comes to calculating the overall connectivity, however, this uncertainty merely manifests itself in the second decimal place, so we consider it negligible.

### 2.3.3. Base Flow Separation
As the rainy season progresses, base flow in the Lutzito stream increases considerably. To minimize the contribution of the base flow component to total event runoff, we separated base flow according to *Dunne and*

*Leopold* [1978]: from the point of initial hydrograph rise, a line that slopes upward at a rate of 0.003667 m$^3$ s$^{-1}$ * catchment area (km$^2$) per hour is drawn and extended until it intercepts the falling limb of the hydrograph. We defined the point of initial hydrograph rise as the first streamflow reading after rainfall started that exceeded the previous reading by a factor of 1.3. This approach resulted in 75 out of the 98 overland-flow monitoring events having a stormflow component. For assessing the influence of connectivity on sediment and total phosphorus yield, the stormflow periods derived in this manner provided the time interval for the calculation of budgets.

### 2.4. Modeling Framework
### 2.4.1. Rationale for an Ensemble Regression Tree Approach
To address our objectives, we needed to (a) identify the most important meteorological conditions for the development of connectivity, (b) predict connectivity for unmonitored events, and (c) derive event-based sediment and total phosphorus yields by interpolation of our intermittent suspended sediment and total phosphorus concentration data (section 2.2.3). Common to all these calculations is the need for handling non-Gaussian data, nonlinear relations between predictors (e.g., rainfall characteristics and antecedent wetness) and response variables (e.g., connectivity and suspended-sediment concentrations), and correlations between predictors (e.g., between total rainfall and rainfall intensity). Only few methods can tackle these aspects simultaneously [*Francke et al.*, 2008; *Zimmermann et al.*, 2012]; among them are multivariate non-parametric regression techniques such as random forest models [*Breiman*, 2001] and Quantile Regression Forest models [*Meinshausen*, 2006].

Quantile Regression Forest (hereafter QRF) builds on random forest (RF) regression tree ensembles. Regression trees, also known as Classification and Regression Trees (CARTs) [*Breiman et al.*, 1984], consist of several decision nodes and are constructed by recursive data partitioning: at each node the calibration data are split into separate subsets so as to reduce the variance of each subset. This procedure continues until a predefined minimum node size has been reached. To avoid overfitting on the calibration data, two principles are to be observed during the construction of the regression trees [*Breiman*, 2001]. First, individual trees of the forest ensemble are grown on a random subset of the calibration data. The procedure of employing only a subset of the calibration data to grow a tree is called "bagging" and the data not used for constructing the trees are termed "out-of-bag data." The idea of bagging is to average many noisy but approximately unbiased models [*Hastie et al.*, 2009]. Second, at each node a random selection of input variables is used to construct the split. The restriction of using only a fraction of predictors reduces the correlation between trees and thus further improves the robustness of the model. In RF, model estimates are based on the mean of all tree predictions, whereas QRF employs the whole distribution of tree predictions [*Meinshausen*, 2006].

For all calculations and model building, we used the software R, version 2.14.0 [*R Development Core Team*, 2011], primarily the packages randomForest [*Liaw and Wiener*, 2002], quantregForest [*Meinshausen*, 2007], and party [*Strobl et al.*, 2008].

### 2.4.2. Modeling Overland-Flow Connectivity and Assessment of Variable Importance
We chose 19 predictor variables to model connectivity derived from our preferred definition, which allowed for one empty OFD between two full ones (cf. section 2.3). We ran our RF and QRF models with the following model parameters: the number of variables selected at each node set to 12, the minimum node size set to 5, and the number of trees set to 5000. Due to the limited number of rainfall events which we monitored for overland-flow occurrence ($n = 98$), we validated our predictions on the out-of-bag data which avoids the need to set aside a fraction of the data for validation [*Breiman*, 2001].

We derived the majority of the predictor variables from the rainfall record (cf. section 2.2.1; for summary statistics of a number of predictors see Table 2), namely the total rain amount per event and the corresponding maximum rainfall intensities, the duration of the event, antecedent precipitation indices spanning 1 day to 4 months, the rainfall before and after the first rainfall peak as surrogates for within-event dynamics. In addition, we computed the day of year as a proxy for the progress of the rainy season. To incorporate available information on soil hydrology, we computed two indices that relate the (near-) surface soil saturated hydraulic conductivity to event-based maximum rainfall intensities. We obtained this $K_s$ data for two soil depths (0–6 cm, $n = 376$ and 6–12 cm, $n = 111$) in the Lutzito catchment in the rainy seasons of 2009 and

2010. The survey of 2010 included the former OFD locations within flow lines (the last year of OF monitoring was 2009); see *Zimmermann et al.* [2013] for further details. For the first index to be used here, we calculated for every rain event the number of times the maximum 5 min rainfall intensity exceeds median $K_s$ at the soil surface (0–6 cm depth) of flow lines. The second index was computed analogously but using spatially distributed $K_s$ data of the near-surface soil (6–12 cm depth).

Random forest facilitates data understanding by comparing candidate predictor variables regarding their impact on predictive accuracy. For this purpose, the random forest algorithm provides variable importance scores [*Breiman*, 2001]. Correlation among predictors complicates the interpretation of these scores because a variable that may appear marginally influential might actually be independent of the response when considered conditional on another variable [*Strobl et al.*, 2008]. To overcome this problem, we used the conditional permutation importance [*Strobl et al.*, 2008] to identify the most important predictor variables for connectivity. This approach distinguishes between the marginal and the conditional effect of a variable; in so doing, the truly influential predictor variables have a higher chance to be detected [*Strobl et al.*, 2008].

### 2.4.3. Modeling Suspended-Sediment and Phosphorus Concentration
The QRF models of suspended-sediment (SSC) and phosphorus concentration (TP) employ 17 predictor variables: 10 variables containing information on antecedent rainfall including short-term (e.g., antecedent 5 min rainfall) and long-term antecedent rainfall (e.g., amount of rainfall in the antecedent weeks), six variables describing antecedent discharge dynamics (antecedent 5 min to several hours prior prediction), and the day of year to capture seasonal trends in the data. We ran the QRF models with the following model parameters: the number of variables selected at each node was set to 8, the minimum node size was set to 5, and the number of trees was set to 1000. We validated the models applying the Nash-Sutcliffe efficiency index [*Nash and Sutcliffe*, 1970]. Because of the comparatively large amount of SSC and TP data we could apply a more elaborate validation: as suggested by *Zimmermann et al.* [2012], we calculated the Nash index for various validation data fractions ranging from 10% to 50% of the total data set and for all possible positions of the validation data with calibration and validation data in temporally contiguous blocks. This procedure avoids arbitrary decisions regarding definition of the size of the validation data set and its location [*Zimmermann et al.*, 2012]. For the final SSC and TP modeling and calculation of event-based sediment and phosphorus yields, we used the full data sets (cf. Table 3). For a more detailed description of the applied QRF models, construction of predictor variables, validation procedures, and calculation of yields we refer to *Zimmermann et al.* [2012].

### 2.4.4. Examining the Relationship Between Connectivity and Catchment Response
Ultimately, we are interested in the relationship between connectivity and the amounts of stormflow, suspended sediment, and phosphorus arriving at the catchment outlet. Because event parameters and antecedent conditions influence connectivity as much as the overall catchment response (e.g., increasing rainfall amounts likely entail higher connectivities as well as larger stormflow volumes), it is preferable to first remove the influence of rainfall depth on catchment response. This was done by dividing an event's stormflow volume, as well as its suspended-sediment and phosphorus yield, by its rainfall amount. For the case of stormflow, this approach yields the event runoff coefficient. To finally illustrate the dependence of the runoff coefficient, the standardized suspended-sediment yield, and the standardized phosphorus yield on connectivity, we fitted nonparametric local regression models.

## 3. Results

### 3.1. Characteristics of Overland-Flow Occurrence and Development of Connectivity in Flow Lines
Hydrograph characteristics, both of streamflow (H1) and of overland-flow delivered by a flow line (H3), highlight the Lutzito catchment's very flashy response to rainfall (Table 4). These characteristics are very similar to reported hydrograph attributes of streamflow and overland flow in the La Cuenca catchment in Peru (compare columns 1 and 3 of our Table 4 with Figure 7 in *Elsenbeer and Vertessy* [2000]), which is not surprising as the La Cuenca catchment is also considered an active hydrological system regarding near-surface processes [*Elsenbeer and Vertessy*, 2000]. The similarity in the timing of streamflow and overland flow (Table 4) furthermore corroborates the argument that overland flow is the dominant flow path in our research catchment (cf. section 2.1).

**Table 4.** Hydrograph Characteristics[a] at Streamgauges H1 and H3

| | Time of Rise[b] (min) | | Lag-to-Peak[c] (min) | | Centroid Lag-to-Peak[d] (min) | |
|---|---|---|---|---|---|---|
| | H1 | H3 | H1 | H3 | H1 | H3 |
| Minimum | 5.0 | 0.0 | 10.0 | 0.0 | 0.0 | −5.0 |
| First quartile | 18.8 | 5.0 | 25.0 | 18.8 | 5.0 | 3.8 |
| Median | 30.0 | 5.0 | 47.5 | 40.0 | 10.0 | 5.0 |
| Third quartile | 86.3 | 15.0 | 107.5 | 101.3 | 16.3 | 11.3 |
| Maximum | 405.0 | 65.0 | 420.0 | 180.0 | 150.0 | 45.0 |
| CI, lower bound[e] | 7.7 | 1.6 | 20.2 | 12.3 | 6.3 | 2.5 |
| CI, upper bound[e] | 52.3 | 8.4 | 74.8 | 67.7 | 13.7 | 7.5 |

[a]For rainfall events that caused stormflow at both streamgauges ($n = 32$).
[b]Time of peak discharge—beginning of hydrograph rise (beginning of hydrograph rise: runoff >1.3 last runoff record for H1 or runoff is at least 0.1 l/s for H3).
[c]Time of peak discharge—beginning of rainfall.
[d]Time of peak discharge—rainfall centroid time (rainfall centroid time: half of the event rainfall has fallen).
[e]95% confidence intervals of the median: median $\pm t_{n-1,\ \alpha/2} * d_F/(1.075\ n^{0.5})$, where $t$ is the value of the $t$-distribution for $\alpha = 0.05$ and $n - 1$ d.f., and $d_F$ is the fourth spread [*Iglewicz*, 1983].

Within flow lines, the temporal frequency of overland-flow occurrence (TF-OF) varies strongly between about 10% and 90% (Figure 3). Interestingly, TF-OF clearly decreases with increasing distance to the intercepting channel, whereas the relationship between TF-OF and all other terrain attributes is weak at best (Figure 3). The preferred occurrence of overland flow at the Lutzito catchment's near-channel locations was observed previously [*Loos and Elsenbeer*, 2011] and matches the progressive decline in the $K_s$ of topsoil in a downslope direction along flow lines [*Zimmermann et al.*, 2013]. Hence, connectivity will be initiated close to the channel network whereupon it sometimes "grows" upstream. This situation, in addition to the importance of microtopography for OF occurrence, suggests that connectivity in the Lutzito catchment is basically an event-dependent expansion of the channel system into the ephemeral and spatially dynamic flow line network (Figure 4), which allows surficial drainage of entire hillslopes under extreme conditions.

### 3.2. Validation of Predictions Using Regression Tree Ensembles

To identify the meteorological controls on connectivity, we used RF/QRF modeling with predictors derived from the rainfall record (cf. section 2.5.2). The validation of the RF and QRF models indicated satisfactory performance, as illustrated by an RMSE of 0.15 (both RF and QRF) and an $R^2$ of 0.80 for RF and 0.78 for QRF models, respectively. Likewise, the QRF model that we used to predict suspended-sediment concentrations performed satisfactorily (Table 5). Because the latter model is based on a comparatively large data set (Table 3), varying the size of calibration and validation data blocks has little influence on the results. In contrast, the QRF model predicting TP concentrations shows a marked decline in model performance (Table 5) if calibration data sets decrease in size (i.e., if we use larger validation data sets). The somewhat lower accuracy of our TP prediction is mainly related to the smaller number of TP data (Table 3).

### 3.3. Influence of Rainfall Characteristics and Antecedent Conditions on Overland-Flow Connectivity

The conditional importance scores that we calculated using an RF model (cf. sections 2.5.1 and 2.5.2) reveal the most important meteorological conditions for the development of connected overland flow (Figure 5). Clearly, the long-term maximum rainfall intensities exert the strongest influence on connectivity. High importance scores are also associated with the total amount of event rainfall and short-term maximum rain intensities. In addition, the frequency at which the maximum 5 min rainfall intensity exceeds the soil saturated hydraulic conductivity of the Lutzito catchment's impeding layer is of some predictive power. The importance of the long-term antecedent conditions, which are represented in the day-of-year index and the cumulated 4 month antecedent precipitation, suggests a relation between connectivity and the stage of the rainy season. In contrast, all short-term antecedent wetness indices have low importance scores. Likewise, the duration of the rainfall event and temporal variations of rainfall within events have no or negligible influence on overland-flow connectivity.

A closer inspection of the relationship between total rainfall in an event and the resulting connectivity reveals interesting aspects. First, there is no rainfall threshold for the development of connectivity; instead,
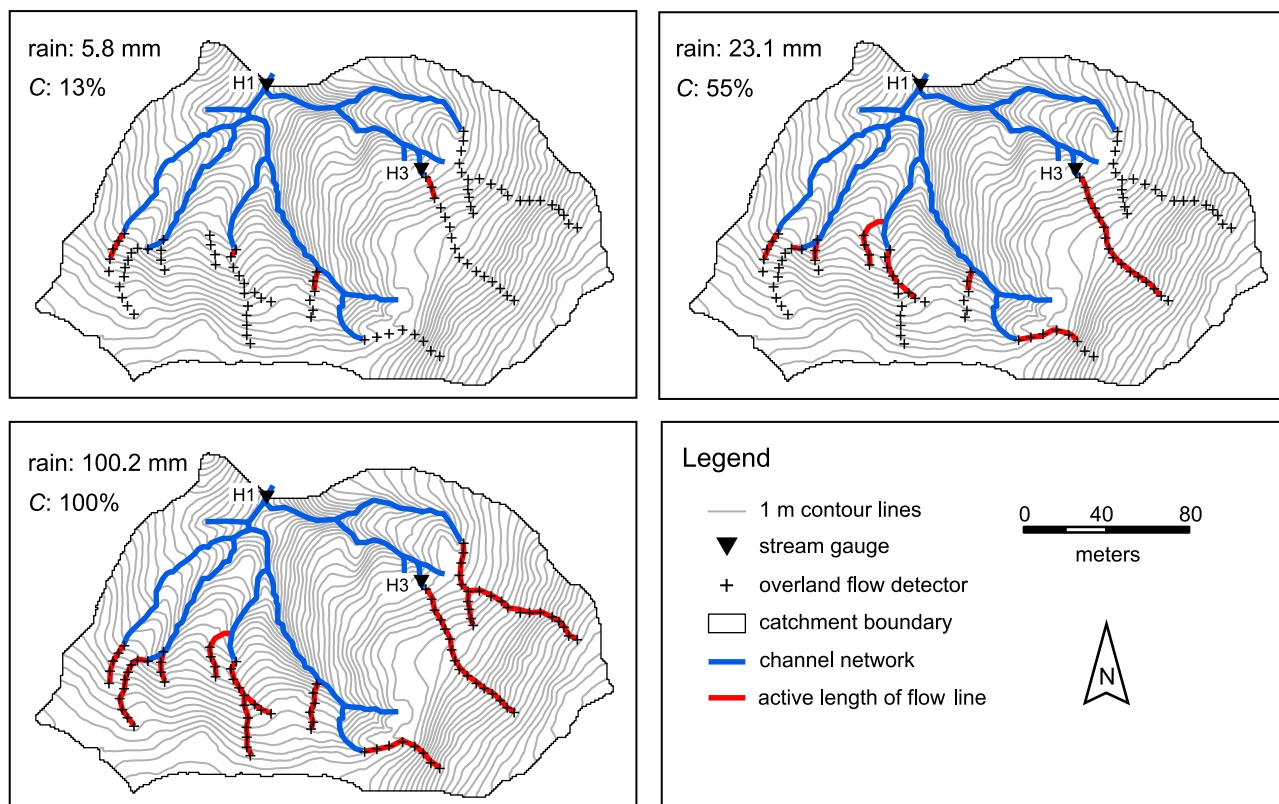
**Figure 4.** Extension of the catchment's drainage network by flow lines during three exemplary chosen rainfall events. These events were associated with overland-flow connectivities of (a) 100%, (b) 13%, and (c) 55%. The active length of each flow line was determined using definition *a*, which is explained in Figure 2.

connectivity rises rapidly with increasing rain amount until full connectivity is reached (Figure 6). This result agrees with our observation that connectivity occurs via flow network expansion (cf. section 3.1). Second, there is considerable scatter in the relationship between rainfall and connectivity; 40 mm rain storms, for instance, are associated with connectivities as low as 40% and up to nearly 100% (Figure 6). This variation can be explained by the long-term antecedent wetness. Rain events following dry antecedent conditions, which mainly occur in the early and midrainy season [*Zimmermann et al.*, 2012], generally require larger and more intense storms for the development of connectivity than do comparable events during wet months (Figure 6). Hence, high-connectivity situations occur primarily in the late rainy season (month of November, Figure 7) but also following a series of storm events at earlier stages of the rainy season (e.g., in August 2009, Figure 7).

In summary, overland-flow connectivity in a given event is influenced mainly by the maximum rainfall intensity, total rain amount, the interplay between intense rainfall and soil permeability, and long-term antecedent wetness. The latter fact complicates the relationship between meteorology and connectivity as the

**Table 5.** Validation of SSC and TP Predictions[a]

| | SSC | | TP | |
|---|---|---|---|---|
| Fraction of Validation Data | Calibration | Validation | Calibration | Validation |
| 0% (full data set) | 0.95 | | 0.92 | |
| 10% | 0.95 | 0.77 | 0.92 | 0.63 |
| 20% | 0.95 | 0.76 | 0.92 | 0.60 |
| 30% | 0.95 | 0.73 | 0.92 | 0.54 |
| 40% | 0.95 | 0.72 | 0.92 | 0.50 |
| 50% | 0.95 | 0.72 | 0.91 | 0.47 |

[a]Nash-Sutcliffe-efficiency indices for all possible positions of contiguous calibration data and various fractions of calibration and validation data; the Nash indices are median values of all positions of validation data for the respective fractions.
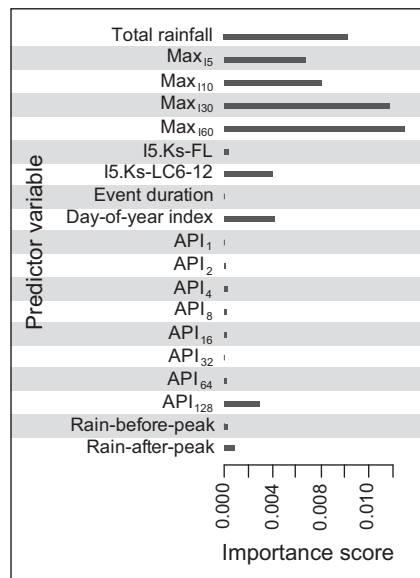
**Figure 5.** Conditional variable importance provided by the Random-Forest algorithm for predicting connectivity from event-based predictor variables, which were derived from the rainfall record. Abbreviations are as follows: $Max_{I5}$, maximum 5 min rainfall intensity; $Max_{I10}$, maximum 10 min rainfall intensity; $Max_{I30}$, maximum 30 min rainfall intensity; $Max_{I60}$, maximum 60 min rainfall intensity; I5.Ks-FL, number of times the 5 min rainfall intensity exceeds the saturated hydraulic conductivity of the surface soil of flow lines; I5.Ks-LC6-12, number of times the 5 min rainfall intensity exceeds the saturated hydraulic conductivity of the Lutzito catchment's soil at 6–12 cm depth; $API_1$, $API_2$, . . .,$API_{128}$, 1, 2, . . .,128 days antecedent precipitation index; rain-before-peak, rainfall amount before first rainfall peak; rain-after-peak, rainfall amount after first rainfall peak.
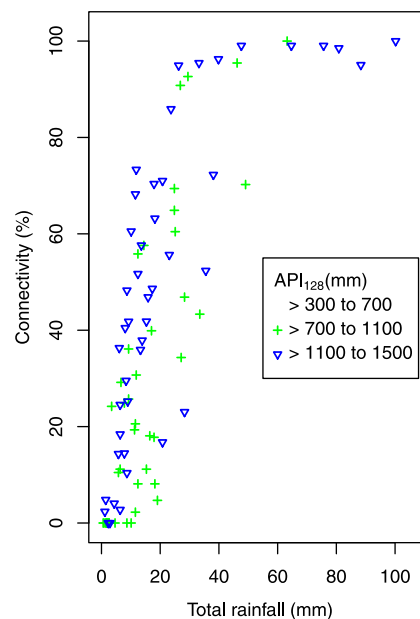


**Figure 6.** Connectivity versus total rainfall. The color code and symbol type, respectively, is adapted to the antecedent-precipitation index calculated for 128 days prior to the respective rainfall event.

particular state of the rainy season determines the storm sizes and intensities necessary for the development of spatially continuous overland flow.

### 3.4. Implications of Connectivity for Catchment Response

First, the runoff coefficients as well as the suspended sediment and the total phosphorus yields are clearly related to connectivity (Figure 8), which implies that the expansion of the channel network by concentrated flow lines is a first-order control of catchment response. Second, the relationships between connectivity and the response variables are apparently subject to nonlinearity (Figure 8), a fact that we attribute, following the typology of the sources of nonlinearity in earth surface systems [*Phillips*, 2003], to thresholds and storage effects. For instance, the contributing area for overland flow differs with storm size because of the spatial pattern of the soil saturated hydraulic conductivity in the Lutzito catchment: rainfall intensities during small events exceed $K_s$ of flow line topsoils at most, whereas those of bigger storms also exceed surface $K_s$ at locations in the vicinity of flow lines [*Zimmermann et al.*, 2013]. This entails a much larger contributing area for the latter situation, which may partly explain the disproportionate increase in outputs as storms get bigger (Figure 8). Likewise, a perched water table presumably develops particularly rapidly during high-connectivity events and persists for a relatively long time. It is further possible that return flow, which we consider an additional source of overland flow in our research catchment, is only activated beyond certain thresholds associated with actual or pre-event meteorological conditions. Finally, larger rainfall depths and intensities have more erosive power, which might enhance sediment and phosphorus detachment and export. While our connectivity index undoubtedly facilitates the understanding of catchment response, there remains considerable unexplained variation, particularly toward the high-connectivity stage (Figure 8). Apart from the difficulties in determining connectivity (cf. section 2.3.2 and uncertainty bands in Figure 8), this is because our index merely characterizes the most extreme catchment state in terms of flow connection, but misses attributes such as the timing and duration of connection, all of which determine the actual quantity and quality of runoff. In addition, our approach does not inform about the source of sediment and TP in high-connectivity situations, because heavy rainfall could mobilize material both from hillslopes and the channels themselves. To investigate this, we determined the TP content of the soil in the Lutzito catchment at 10 randomly selected locations and of channel side walls ($n = 9$). Comparatively low TP concentrations in the stream channel compared to
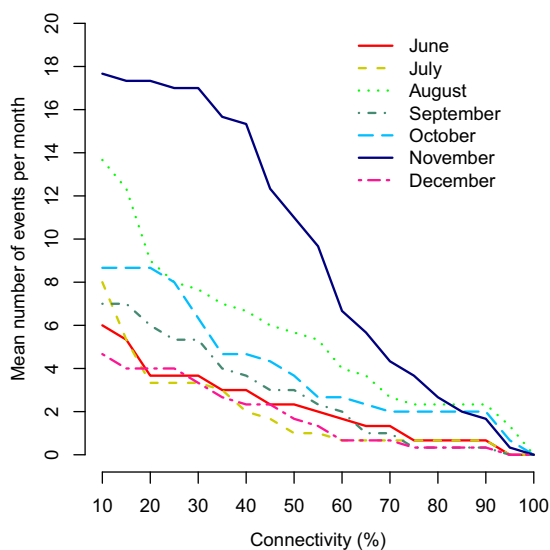
**Figure 7.** Mean number of events per month exceeding given stages of overland-flow connectivity in the Lutzito catchment during the rainy seasons 2007–2009. We used the QRF model to predict connectivity of unmonitored events.

the soil, particularly to the soil surface (Figure 9), favor the hillslopes as the main source of TP during high-connectivity rainfall events.

## 4. Discussion

### 4.1. Establishment and Controls of Hydrological Connectivity

Our results demonstrate that the preferred occurrence of overland flow in the near-channel area of concentrated flow lines entails an immediate coupling of hillslopes and channels without the need to exceed certain critical rainfall depths. The missing rainfall threshold might at first appear surprising, since rainfall interception by the forest canopy is particularly large for small events [e.g., *Helvey and Patric*, 1965]. The situation changes, however, if we consider the complexity in the relationship between event parameters and interception loss; for instance, interception loss during a small storm on a wet canopy will differ from that of an equally sized event hitting a dry canopy.

In general, the absence of a rainfall threshold distinguishes hillslope-channel coupling at our site not only from subsurface-flow connectivity [*Ocampo et al.*, 2006; *McGuire and McDonnell*, 2010] but probably also from hydrological connectivity based on infiltration-excess overland flow, because in the latter case the filling of storage depressions is required before the excess water runs off [*Darboux et al.*, 2002]. Neither storm duration nor within-event variations of rainfall influence connectivity in the Lutzito catchment (Figure 5). This is in contrast to observations in semiarid areas, where reinfiltration of infiltration-excess overland flow during short events occurs [*Reaney et al.*, 2007], or where a wetting-up of the catchment is prerequisite for the establishment of connectivity [*Bracken and Croke*, 2007].

The importance of the stage of rainy season (Figure 5) for connectivity reflects the soil conditions of the Lutzito catchment: soil cracks are abundant in the dry season or during pronounced dry spells in the rainy season (Figure 1g), when only small amounts of overland flow reach the channel network [*Zimmermann et al.*, 2012]. At this point, it is worth mentioning that soil cracking is widespread in the Panama Canal area [*Hendrickx et al.*, 2005; *Hassler et al.*, 2011]. As the rainy season progresses, a constant increase of the degree of saturation (i.e., wetness) promotes connectivity for modest rain events (Figure 6). This observation is consistent with the finding of *Bonell et al.* [1979] that only small amounts of rainfall were required to initiate SOF in the hydrologically similar South Creek catchment, which they attributed to perpetual near-saturated conditions in the wet season. Apart from the influence of soil moisture on the development of connectivity, soil cover by leaf litter might also exert some control on connectivity in the Lutzito catchment. Because litter fall peaks in the dry season when decomposition rates are low, the amount of leaf litter on the soil surface is greater in the early than in the late rainy season [*Wieder and Wright*, 1995]. The existence of litter on the forest floor increases rainfall interception [*Marin et al.*, 2000; *Park et al.*, 2010] and may also impose barriers to surface runoff [*Sayer*, 2006], both of which likely impede overland-flow connectivity in the early wet-season (Figure 1e). In contrast, flow lines are essentially bare of leaf litter in the late rainy season (Figures 1d and 1f). Hence, a combination of factors, most likely related to seasonal soil moisture variation and phenology, account for the long-term antecedent-wetness control on overland-flow connectivity in the Lutzito catchment. Of course, seasonal controls on connectivity in temperate areas dominated by subsurface flow also exist, e.g., related to increases in catchment wetness during snowmelt [*Jensco et al.*, 2009].
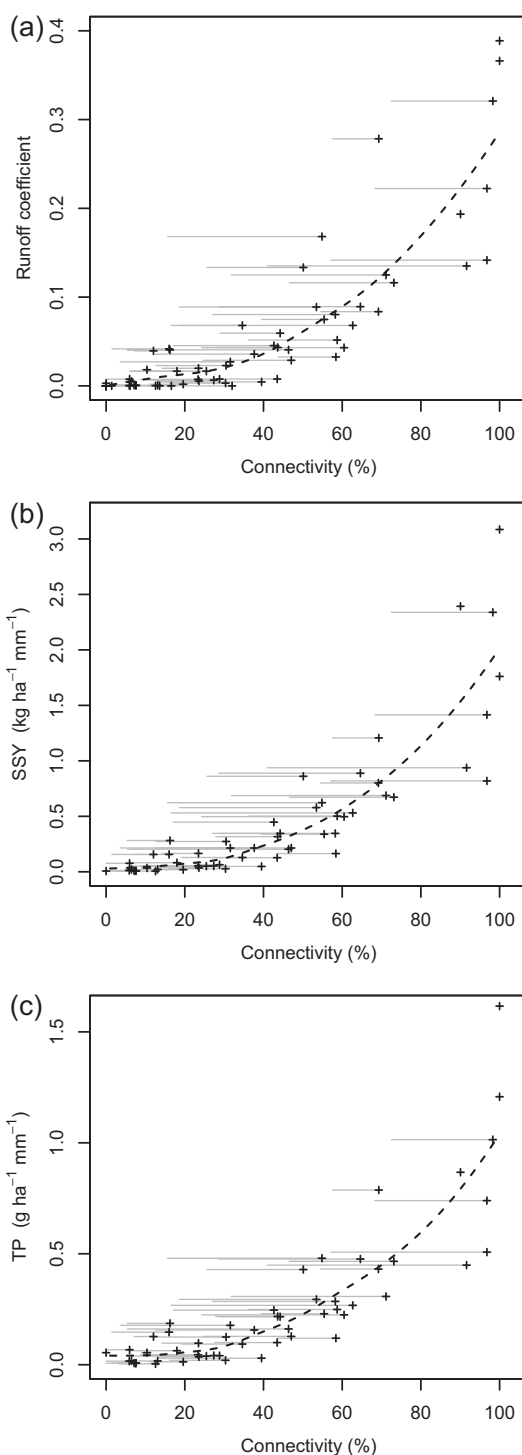
**Figure 8.** Dependence of stormflow volume, suspended-sediment yield, and phosphorus yield, all of which were measured at the catchment outlet (stream gauge H1, Figure 1c) and standardized by total rainfall, on connectivity. Uncertainty in deriving the overall connectivity is indicated by the horizontal gray lines: crosses refer to connectivity calculated with the preferred active-length definition *a* and the left end of the line is defined by the connectivity index computed with the alternative definition *b* (see Figure 2 for details). The dotted lines display nonparametric local regression models that we fitted to the relationships between connectivity as obtained with the active-length definition *a* and the response variables.

In summary, our results support the claim (cf. section 1) that the dynamic component of connectivity is specific to the system under study. This suggests that knowledge about a catchment's main runoff mechanisms should suffice for educated guesses about necessary antecedent conditions and important rainfall parameters for the establishment of connectivity between hillslopes and streams.

### 4.2. Connectivity: What Is It Good For?

Our connectivity index explains catchment behavior to a large degree, with the remaining scatter most likely due to missing information about the actual volume of overland flow. As stated in *Jensco et al.* [2009], connectivity thresholds, duration of connection and amount of water flowing through certain landscape elements all control the magnitude of runoff. However, incorporating all these facets into an assessment of connectivity would come at substantial cost. Hence, instead of accumulating ever-more detailed information with limited transferability, we expect greatest benefit of the connectivity concept from its application, which we outline below.

First, connectivity assessments are useful in hydrological modeling, because hillslope flow paths represented in a model need to be routed to the stream network. An example of a hillslope-scale model that implicitly accounts for connectivity of infiltration-excess overland flow is the Connectivity of Runoff Model (CRUM) developed by *Reaney et al.* [2007]. *Mueller et al.* [2007] showed that model performance improved when overland-flow connectivity was sufficiently represented in the model structure. In that case, a comparatively simple index of HOF connectivity (i.e., the spatial distribution of vegetation cover) produced similar results to the much more data-intensive conditional simulation of estimated saturated hydraulic conductivity and friction factors [*Mueller et al.*, 2007]. If we wanted to represent overland-flow connectivity in a rainfall-runoff model for Lutzito and similar catchments, one possibility would be to incorporate realistic spatial fields of $K_s$ based on
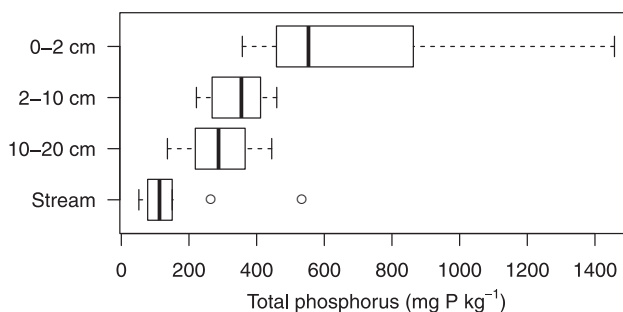
**Figure 9.** Boxplot comparison of total phosphorus content at three soil depths measured at 10 randomly selected sites in the Lutzito catchment and at nine locations within the catchment's channel system. The boxes contain the middle 50% of the data, that is, data within the interquartile range; the vertical thick lines in the boxes refer to the median. The whiskers extend to a maximum distance of 1.5 times the interquartile range from the first or third quartile, respectively. Data points beyond this distance are shown as circles.

topographic attributes [*Zimmermann et al.*, 2013]. Another option is to build a flexible box model [*McDonnell*, 2003], where hillslopes and the channel network are coupled according to the described relationships between storm characteristics, connectivity, and catchment response.

Second, we advocate using the connectivity concept for catchment classification and management. *Jensco et al.* [2009] provided a successful example: they first linked the hillslope-riparian-stream (HRS) connection of groundwater flow to runoff response, and then established a relationship between connectivity and a topographic metric, which eventually allowed them to use connectivity as a means of runoff prediction at unmeasured locations. Classifications like this help identify parts of larger watersheds that are particularly important with respect to flow path connectivity. Attempts to develop metrics for connectivity strive for the same goal, but use a top-down approach: first, a connectivity metric is developed, which is then assessed by its ability to predict catchment response [*Ali and Roy*, 2010; *Lane et al.*, 2009; *Mayor et al.*, 2008]. The difficulty lies in representing connectivity in a meaningful way; we argue that (field) knowledge about the system under consideration is essential to guide the "shopping for hydrologically representative connectivity metrics" [*Ali and Roy*, 2010]; it definitely helps if the structural aspect of connectivity [*Wainwright et al.*, 2011] can be assessed a priori.

Other disciplines likewise recognize the potential of the connectivity concept to serve as a rapid assessment tool: in conservation planning, analyses of landscape networks are suggested as suitable for a rough prioritization of habitat resources [*Urban and Keitt*, 2001]. As to hydrological connectivity in our undisturbed study area, the existence of flow lines is a sign of active surficial processes that, as we have shown, are responsible for the catchment's fast and intense response to rainfall (Figures 6–8). Hence, measures like flow line density should be useful for building classes of catchment responsiveness, which could be incorporated into a HOST framework (hydrology of soil types) [*Boorman et al.*, 1995], or be used to scale, for example, retention factors of grid cells within grid-based hydrological models. At this point, it is important to note that field investigations might be more suitable for building such a classification than digital elevation models because of the often unknown and spatially variable thresholds for channel initiation. In addition, the spatial scale of microtopography, which is important in our case, is beyond the resolution of standard elevation models [*Loos and Elsenbeer*, 2011]. Finally, a map of expected catchment behavior for a larger region (e.g., the forested part of the Panama Canal Watershed) would provide an important tool for watershed management; for instance, in inherently highly active systems land use may well affect sediment export and solute fluxes stronger than it does in well-buffered systems [*Hayhoe et al.*, 2011]. Thus, the application of the connectivity concept as a rapid assessment tool in hydrology appears promising, particularly in data-sparse regions where even basic information such as soil maps or digital elevation models often is unavailable.

## 5. Conclusions

The research questions posed initially can be answered as follows:

(1) In the study area, an overland-flow prone rain forest catchment, connectivity develops by the upslope expansion of the drainage network along flow lines from channel heads towards the divide. Under extremely wet conditions, the "belt of no overland flow" disappears in places, at which point the divide becomes connected to the channel system.

(2) Rainfall total, maximum rainfall intensity, and seasonal variations of antecedent wetness control the development of connectivity, whereas short-term antecedent wetness and within-event rainfall variability do not matter.

(3) Connectivity influences stormflow, suspended-sediment, and phosphorus yields in a nonlinear fashion, which we attribute to contributing areas growing disproportionately after connectivity exceeds a certain threshold. A connectivity >40% triggers an exponential increase of the runoff coefficient and an exponentially increasing efficiency of suspended-sediment and phosphorus export.

Based on the important role of connectivity in controlling catchment responses, we envision various applications of the connectivity concept, e.g., in hydrological modeling by informing about the nature and variability of hillslope-channel coupling, and in rapid hydrological assessment as a tool for classification with regard to catchments' responsiveness.

## References

Ali, G. A., and A. G. Roy (2010), Shopping for hydrologically representative connectivity metrics in a humid temperate forested catchment, *Water Resour. Res.*, *46*, W12544, doi:10.1029/2010WR009442.

Baillie, I., H. Elsenbeer, F. Barthold, R. Grimm, and R. Stallard (2007), Semi-detailed soil survey of Barro Colorado Island, Panama. Soil Report [online]. [Available at http://biogeodb.stri.si.edu/bioinformatics/bci_soil_map/index.php, verified 22 September 2010.]

Bonell, M., D. A. Gilmour, and D. F. Sinclair (1979), Statistical method for modeling the fate of rainfall in a tropical rainforest catchment, *J. Hydrol.*, *42*, 251–267, doi:10.1016/0022-1694(79)90050-7.

Boorman, D. B., J. M. Hollis, and A. Lilly (1995), Hydrology of soil types: A hydrologically-based classification of the soils of the United Kingdom, *Rep. 126*, Inst. of Hydrol., Wallingford.

Bracken, L. J., and J. Croke (2007), The concept of hydrological connectivity and its contribution to understanding runoff-dominated geomorphic systems, *Hydrol. Processes*, *21*, 1749–1763, doi:10.1002/hyp.6313.

Brauman, K. A., G. C. Daily, T. K. Duarte, and H. A. Mooney (2007), The nature and value of ecosystem services: An overview highlighting hydrologic services, *Annu. Rev. Environ. Resour.*, *32*, 67–98, doi:10.1146/annurev.energy.32.031306.102758.

Breiman, L. (2001), Random forests, *Mach. Learn.*, *45*, 5–32, doi:10.1023/A:1010933404324.

Breiman, L., J. Friedman, R. Olshen, and C. Stone (1984), *Classification and Regression Trees*, Wadsworth, Belmont, Calif.

Brunsden, D., and J. B. Thornes (1979), Landscape sensitivity and change, *Trans. Inst. Br. Geogr.*, *4*, 463–486.

Buttle, J. M., and D. S. Turcotte (1999), Runoff processes on a forested slope on the Canadian shield, *Nordic Hydrol.*, *30*, 1–20, doi:10.2166/nh.1999.001.

Darboux, F., P. Davy, and C. Gascuel-Odoux (2002), Effect of depression storage capacity on overland-flow generation for rough horizontal surfaces: Water transfer distance and scaling, *Earth Surf. Processes Landforms*, *27*, 177–191, doi:10.1002/esp.312.

Dunne, T., and L. B. Leopold (1978), *Water in Environmental Planning*, W. H. Freeman, San Francisco.

Elsenbeer, H., and R. A. Vertessy (2000), Stormflow generation and flowpath characteristics in an Amazonian rainforest catchment, *Hydrol. Processes*, *14*, 2367–2381, doi:10.1002/1099-1085(20001015)14:14<2367::aid-hyp107>3.0.co;2-h.

FAO (1998), World reference base for soils, World Soil Resour. *Rep. 84*, Food and Agric. Organ. of U. N., Rome.

Foster, R. B., and N. V. L. Brokaw (1982), Structure and history of the vegetation of Barro Colorado Island, in *The Ecology of a Tropical Forest: Seasonal Rhythms and Long Term Changes*, edited by E. G. Leigh, S. A. Rand, and D. M. Windsor, pp. 67–81, Smithson. Inst., Washington, D. C.

Francke, T., J. A. Lopez-Tarazon, and B. Schroeder (2008), Estimation of suspended sediment concentration and yield using linear models, random forests and quantile regression forests, *Hydrol. Processes*, *22*, 4892–4904, doi:10.1002/hyp.7110.

Frey, M. P., M. K. Schneider, A. Dietzel, P. Reichert, and C. Stamm (2009), Predicting critical source areas for diffuse herbicide losses to surface waters: Role of connectivity and boundary conditions, *J. Hydrol.*, *365*, 23–36, doi:10.1016/j.jhydrol.2008.11.015.

Godsey, S., H. Elsenbeer, and R. Stallard (2004), Overland flow generation in two lithologically distinct rainforest catchments, *J. Hydrol.*, *295*, 276–290, doi:10.1016/j.jhydrol.2004.03.014.

Gomi, T., Y. Asano, T. Uchida, Y. Onda, R. C. Sidle, S. Miyata, K. Kosugi, S. Mizugaki, T. Fukuyama, and T. Fukushima (2010), Evaluation of storm runoff pathways in steep nested catchments draining a Japanese cypress forest in central Japan: A geochemical approach, *Hydrol. Processes*, *24*, 550–566, doi:10.1002/hyp.7550.

Grimm, R., T. Behrens, M. Marker, and H. Elsenbeer (2008), Soil organic carbon concentrations and stocks on Barro Colorado Island—Digital soil mapping using Random Forests analysis, *Geoderma*, *146*, 102–113, doi:10.1016/j.geoderma.2008.05.008.

Hassler, S. K., B. Zimmermann, M. van Breugel, J. S. Hall, and H. Elsenbeer (2011), Recovery of saturated hydraulic conductivity under secondary succession on former pasture in the humid tropics, *For. Ecol. Manage.*, *261*, 1634–1642, doi:10.1016/j.foreco.2010.06.031.

Hastie, T., R. Tibshirani, and J. Friedman (2009), *The Elements of Statistical Learning*, pp. 587–604, Springer, New York, doi:10.1007/b94608_15.

Hayhoe, S. H., C. Neill, S. Porder, R. McHorney, P. Lefebvre, M. T. Coe, H. Elsenbeer, and A. V. Krusche (2011), Conversion to soy on the Amazonian agricultural frontier increases streamflow without affecting stormflow dynamics, *Global Change Biol.*, *17*, 1821–1833, doi:10.1111/j.1365-2486.2010.02392.x.

Helvey, J. D., and J. H. Patric (1965), Canopy and litter interception of rainfall by hardwoods of Eastern United States, *Water Resour. Res.*, *1*, 193–206, doi:10.1029/WR001i002p00193.

Hendrickx, J. M. H., D. Vega, J. B. J. Harrison, L. E. C. Gobbetti, P. Rojas, and T. W. Miller (2005), Hydrology of hillslope soils in the Upper Río Chagres watershed, Panama, in *The Rio Chagres, Panama: A Multidisciplinary Profile of a Tropical Watershed*, edited by R. S. Harmon, pp. 113–138, Water Sci. and Technol. Lib., Springer, Dordrecht, Netherlands.

Hölzel, H., and B. Diekkrüger (2012), Predicting the impact of linear landscape elements on surface runoff, soil erosion, and sedimentation in the Wahnbach catchment, Germany, *Hydrol. Processes*, *26*, 1642–1654, doi:10.1002/hyp.8282.

Iglewicz, B. (1983), Robust scale estimators and confidence intervals for location, in *Understanding Robust and Exploratory Data analysis*, edited by D. C. Hoaglin, F. Mosteller, and J. W. Tukey, pp. 404–429, John Wiley, New York.

Jencso, K. G., B. L. McGlynn, M. N. Gooseff, S. M. Wondzell, K. E. Bencala, and L. A. Marshall (2009), Hydrologic connectivity between landscapes and streams: Transferring reach-and plot-scale understanding to the catchment scale, *Water Resour. Res.*, *45*, W04428, doi: 10.1029/2008WR007225.

Kenoyer, L. A. (1929), General and successional ecology of the lower tropical rainforest at Barro Colorado Island, Panama, *Ecology*, *10*, 201–222.

Kinner, D. A., and R. F. Stallard (2004), Identifying storm flow pathways in a rainforest catchment using hydrological and geochemical modelling, *Hydrol. Processes*, *18*, 2851–2875, doi:10.1002/hyp.1498.

Kirkby, M., J. Callan, D. Weyman, and J. Wood (1976), Measurement and modelling of dynamic contributing areas in very small catchments, *Working Pap. 167*, 39 pp., Sch. of Geogr., Univ. of Leeds, Leeds, U. K.

Lane, S. N., S. M. Reaney, and A. L. Heathwaite (2009), Representation of landscape hydrological connectivity using a topographically driven surface flow index, *Water Resour. Res.*, *45*, W08423, doi:10.1029/2008WR007336.

Liaw, A., and M. Wiener (2002), Classification and regression by randomForest, *R News*, *2/3*, 18–22.

Loos, M., and H. Elsenbeer (2011), Topographic controls on overland flow generation in a forest—An ensemble tree approach, *J. Hydrol.*, *409*, 94–103, doi:10.1016/j.jhydrol.2011.08.002.

Marin, C. T., I. W. Bouten, and S. Dekker (2000), Forest floor water dynamics and root water uptake in four forest ecosystems in northwest Amazonia, *J. Hydrol.*, *237*, 169–183.

Mayor, A. G., S. Bautista, E. E. Small, M. Dixon, and J. Bellot (2008), Measurement of the connectivity of runoff source areas as determined by vegetation pattern and topography: A tool for assessing potential water and soil losses in drylands, *Water Resour. Res.*, *44*, W10423, doi:10.1029/2007WR006367.

McDonnell, J. J. (2003), Where does water go when it rains? Moving beyond the variable source area concept of rainfall-runoff response, *Hydrol. Processes*, *17*, 1869–1875, doi:10.1002/hyp.5132.

McGuire, K. J., and J. J. McDonnell (2010), Hydrological connectivity of hillslopes and streams: Characteristic time scales and nonlinearities, *Water Resour. Res.*, *46*, W10543, doi:10.1029/2010WR009341.

Meinshausen, N. (2006), Quantile regression forests, *J. Mach. Learn. Res.*, *7*, 983–999.

Meinshausen, N. (2007), quantregForest: Quantile regression forests, *R package version 0.2-2*.

Michaelides, K., and A. Chappell (2009), Connectivity as a concept for characterising hydrological behaviour, *Hydrol. Processes*, *23*, 517–522, doi:10.1002/hyp.7214.

Michaelides, K., and J. Wainwright (2002), Modelling the effects of hillslope-channel coupling on catchment hydrological response, *Earth Surf. Processes Landforms*, *27*, 1441–1457, doi:10.1002/esp.440.

Mueller, E. N., J. Wainwright, and A. J. Parsons (2007), Impact of connectivity on the modeling of overland flow within semiarid shrubland environments, *Water Resour. Res.*, *43*, W09412, doi:10.1029/2006WR005006.

Nash, J. E., and J. V. Sutcliffe (1970), River flow forecasting through conceptual models. Part I: A discussion of principles, *J. Hydrol.*, *10*, 282–290.

Ocampo, C. J., M. Sivapalan, and C. Oldham (2006), Hydrological connectivity of upland-riparian zones in agricultural catchments: Implications for runoff generation and nitrate transport, *J. Hydrol.*, *331*, 643–658, doi:10.1016/j.jhydrol.2006.06.010.

Park, A., P. Friesen, and A. A. S. Serrud (2010), Comparative water fluxes through leaf litter of tropical plantation trees and the invasive grass *Saccharum spontaneum* in the Republic of Panama, *J. Hydrol.*, *383*, 167–178, doi:10.1016/j.jhydrol.2009.12.033.

Phillips, J. D. (2003), Sources of nonlinearity and complexity in geomorphic systems, *Prog. Phys. Geogr.*, *27*, 1–23, doi:10.1191/0309133303pp340ra.

R Development Core Team (2011), *R: A Language and Environment for Statistical Computing*, R Found. for Stat. Comput., Vienna.

Reaney, S. M., L. J. Bracken, and M. J. Kirkby (2007), Use of the Connectivity of Runoff Model (CRUM) to investigate the influence of storm characteristics on runoff generation and connectivity in semi-arid areas, *Hydrol. Processes*, *21*, 894–906, doi:10.1002/hyp.6281.

Rowland, A. P., and P. M. Haygarth (1997), Determination of total dissolved phosphorus in soil solutions. *J. Environ. Qual.*, *26*, 410–415.

Sayer, E. J. (2006), Using experimental litter manipulation to assess the roles of leaf litter in the functioning of forest ecosystems, *Biol. Rev.*, *81*, 1–31, doi:10.1017/S1464793105006846.

Sayer, A. M., R. P. D. Walsh, and K. Bidin (2006), Pipeflow suspended sediment dynamics and their contribution to stream sediment budgets in small rainforest catchments, Sabah, Malaysia, *For. Ecol. Manage.*, *224*, 119–134, doi:10.1016/j.foreco.2005.12.012.

Sen, S., P. Srivastava, J. H. Dane, K. H. Yoo, and J. N. Shaw (2010), Spatial-temporal variability and hydrologic connectivity of runoff generation areas in a North Alabama pasture-implications for phosphorus transport, *Hydrol. Processes*, *24*, 342–356, doi:10.1002/hyp.7502.

Soil Survey Staff (2006), *Keys to Soil Taxonomy*, 10th ed., U.S. Dep. of Agric., Washington, D. C.

Strobl, C., A. L. Boulesteix, T. Kneib, T. Augustin, and A. Zeileis (2008), Conditional variable importance for random forests, *BMC Bioinformatics*, *9*, 307, doi:10.1186/1471-2105-9-307.

Tromp-van Meerveld, H. J., and J. J. McDonnell (2006a), Threshold relations in subsurface stormflow. 1: A 147-storm analysis of the Panola hillslope, *Water Resour. Res.*, *42*, W02410, doi:10.1029/2004WR003778.

Tromp-van Meerveld, H. J., and J. J. McDonnell (2006b), Threshold relations in subsurface stormflow. 2: The fill and spill hypothesis, *Water Resour. Res.*, *42*, W02411, doi:10.1029/2004WR003800.

Urban, D., and T. Keitt (2001), Landscape connectivity: A graph-theoretic perspective, *Ecology*, *82*, 1205–1218, doi:10.1890/0012-9658(2001)082[1205:lcagtp]2.0.co;2.

Wainwright, J., L. Turnbull, T. G. Ibrahim, I. Lexartza-Artza, S. F. Thornton, and R. E. Brazier (2011), Linking environmental regimes, space and time: Interpretations of structural and functional connectivity, *Geomorphology*, *126*, 387–404, doi:10.1016/j.geomorph.2010.07.027.

Wieder, R. K., and S. J. Wright (1995), Tropical forest litter dynamics and dry season irrigation on Barro Colorado Island, Panama, *Ecology*, *76*, 1971–1979, doi:10.2307/1940727.

Woodring, W. (1958), Geology of Barro Colorado Island, Canal Zone, *Smithson. Misc. Collect.*, *135*(3), 1–39.

Ziegler, A. D., R. A. Sutherland, and T. W. Giambelluca (2001), Acceleration of Horton overland flow and erosion by footpaths in an upland agricultural watershed in northern Thailand, *Geomorphology*, *41*, 249–262.

Zimmermann, A., B. Zimmermann, and H. Elsenbeer (2009), Rainfall redistribution in a tropical forest: Spatial and temporal patterns, *Water Resour. Res.*, *45*, W11413, doi:10.1029/2008WR007470.

Zimmermann, A., T. Francke, and H. Elsenbeer (2012), Forests and erosion: Insights from a study of suspended-sediment dynamics in an overland flow-prone rainforest catchment, *J. Hydrol.*, *428–429*, 170–181, doi:10.1016/j.jhydrol.2012.01.039.

Zimmermann, A., D. S. Schinn, T. Francke, H. Elsenbeer, and B. Zimmermann (2013), Uncovering patterns of near-surface saturated hydraulic conductivity in an overland flow-controlled landscape, *Geoderma*, *195–196*, 1–11, doi:10.1016/j.geoderma.2012.11.002.